



Institut für Numerische Simulation

Rheinische Friedrich-Wilhelms-Universität Bonn

Endenicher Allee 19b • 53115 Bonn • Germany
phone +49 228 73-69828 • fax +49 228 73-69847
www.ins.uni-bonn.de

B. Fuchs, J. Garcke

Simplex Stochastic Collocation for
Piecewise Smooth Functions with Kinks

INS Preprint No. 1901

February 2019

Simplex Stochastic Collocation for Piecewise Smooth Functions with Kinks

Barbara Fuchs¹ and Jochen Garcke^{1,2,3}

¹Fraunhofer SCAI, Sankt Augustin, Germany

²Fraunhofer Center for Machine Learning, Sankt Augustin, Germany

³Institut für Numerische Simulation, Universität Bonn, Germany

February 5, 2019

Abstract Most approximation methods in high dimensions exploit smoothness of the function being approximated. These methods provide poor convergence results for non-smooth functions with kinks. For example, such kinks can arise in the uncertainty quantification of quantities of interest for gas networks. This is due to the regulation of the gas flow, pressure, or temperature. But, one can exploit that for each sample in the parameter space it is known if a regulator was active or not, which can be obtained from the result of the corresponding numerical solution. This information can be exploited in a stochastic collocation method. We approximate the function separately on each smooth region by polynomial interpolation and obtain an approximation to the kink. Note that we do not need information about the exact location of kinks, but only an indicator assigning each sample point to its smooth region. We obtain a global order of convergence of $(p + 1)/d$, where p is the degree of the employed polynomials and d the dimension of the parameter space.

1 Introduction

In many applications in engineering and science the input data of meta models or simulations is uncertain. These uncertainties can arise, e.g. in the geometry, boundary conditions, or model coefficients. One is often interested in how these uncertainties influence some specific output variables also called quantities of interest (QoI). For such an uncertainty quantification (UQ) we need methods to approximate and integrate high dimensional functions. In the case of smooth functions there are several methods such as (adaptive) sparse grids, Galerkin methods, Polynomial chaos expansion or quasi Monte Carlo methods [19]. For discontinuous functions methods exist such as adaptive sparse grids [8], Voronoi piecewise surrogate models (VPS) [15] or simplex stochastic collocation (SSC) [20, 21, 22]. The ideas behind VPS and SSC are similar, in both cases the function is locally approximated by piecewise polynomials either on Voronoi cells or on simplices resulting from a Delaunay triangulation. In VPS a jump in the function is detected if the difference in the function values between neighboring cells exceeds a user defined threshold, while SSC detects a jump not directly but by observing the resulting oscillations. Other alternative approaches for handling discontinuities include enriching the polynomial approximation basis, which generally requires some a priori knowledge of the discontinuity, domain decomposition, also known as multi-element

approximations in this context, or discontinuity detection algorithms, see e.g. [2, 16] for current references. Note that non-smooth functions with kinks can be smoothed by integration [5, 6] over one dimension if the location of the kink is known.

In the simulation of gas networks the solution functions are continuous, but not globally differentiable due to human intervention through the use of control valves, compressors, or heaters. Kinks in a function arise at hyper-surfaces where the function is not continuously differentiable. The idea of simplex stochastic collocation [20, 21, 22] is to approximate a function f by a piecewise polynomial interpolation on simplices. Since polynomial interpolation gets oscillatory near discontinuities, one ensures that the approximation is local extremum conserving, i.e. maximum and minimum of the approximation in any simplex must be attained at its vertices, otherwise the polynomial degree is decreased by one [20]. This condition results in a fine discretization near discontinuities and a coarser discretization at smooth regions. We evaluated the original approach for functions with kinks, but were not able to reach the desired convergence rates, i.e. by increasing the polynomial degree the approximation of a kink could not be improved.

Based on the original simplex stochastic collocation, we introduce a new approach by taking advantage of additional knowledge. In particular, we assume to know on which side of the kink a specific collocation point is situated. This enables us to approximate the function on each side of the kink separately. In doing so, we can improve the convergence rate significantly by not wasting sampling points near the kink. This assumption is motivated by the uncertainty quantification for gas networks. Although we have no information regarding the location of a kink, we know which elements of the gas network cause kinks. After simulating the gas flow for a specific combination of uncertain parameters, we know whether the kink inducing elements are active or not. In the case of a control valve we only need to check if the outgoing pressure lies below the preset pressure p_{set} or equals it.

The paper is organized as follows. In the second section we introduce the SSC method in general and our modifications for piecewise smooth functions with kinks. In addition, we discuss where to sample a new point in order to refine a simplex, how to estimate the error, and if it is possible to refine multiple simplices at once. In the third section we quantify the uncertainty in a particular node of a gas network caused by uncertain input data by applying SSC to calculate the expected pressure.

2 Simplex Stochastic Collocation

We now introduce the approach of simplex stochastic collocation following [20, 21, 22]. Let $\Omega = [0, 1]^d$ and $f : \Omega \rightarrow \mathbb{R}$ be a continuous function. We first discuss the Delaunay triangulation of a given set of n uniformly distributed sampling points \mathbf{x}_i , which divides the parameter space Ω into m disjoint simplices T_j , before considering refinement strategies. Note that the sampling points always include the corners of Ω . Each simplex T_j is defined by its $d + 1$ vertices $\mathbf{x}_{i_j,l}$, with $i_{j,l} \in \{1, \dots, n\}$ and $l \in \{0, \dots, d\}$.

2.1 The Original SSC

Let $f \in \mathcal{C}^0(\Omega)$ be a continuous function that we approximate by m piecewise polynomial functions $g_j(\mathbf{x})$ defined on simplex T_j

$$f(\mathbf{x}) \approx \sum_{i=1}^m g_i(\mathbf{x}) \mathbb{1}_{T_i}.$$

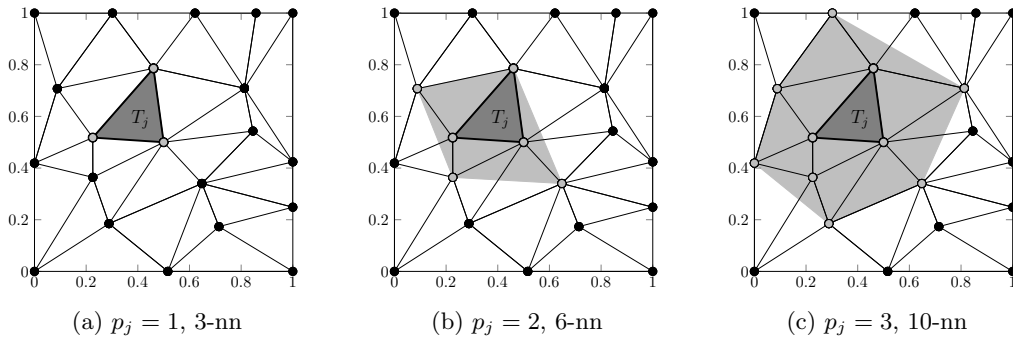


Figure 1: Shown are the Delaunay triangulation of $n = 20$ sampling points and the nearest neighbor stencils S_j (light gray) for simplex T_j (dark gray) for polynomial degrees $p_j = 1, 2, 3$.

The polynomials g_j are defined as

$$g_j(\mathbf{x}) = \sum_{k=1}^{N_j} c_{j,k} \psi_{j,k}(\mathbf{x}),$$

where $\psi_{j,k}$ are some appropriate basis polynomials, $c_{j,k}$ the corresponding coefficients, and $N_j = (d+p_j)!/(d!p_j!)$ the number of degrees of freedom, with $p_j \leq p_{\max}$ the local polynomial degree. Note that in our numerical experiments we use the monomial basis. The polynomial approximation $g_j(\mathbf{x})$ in T_j is constructed by interpolating $f(\mathbf{x})$ in a stencil

$$S_j = \{\mathbf{x}_{i_j,0}, \dots, \mathbf{x}_{i_j,N_j}\}$$

consisting of N_j points out of the sampling points \mathbf{x}_i . These points are chosen to be the nearest neighbors to simplex T_j based on the Euclidean distance to its center of mass. Since in the case of long and flat simplices not necessarily all of its vertices belong to the set of nearest neighbors, we always include the $d+1$ simplex vertices in S_j . Thus, we ensure that our approximation is exact at all sampling points. See Figure 1 for different nearest neighbor stencils of simplex T_j corresponding to polynomial degrees $p_j = 1, 2, 3$. If the interpolation problem is not uniquely solvable we reduce the polynomial degree p_j successively by one until the solution is unique. To avoid oscillations in an approximation $g_j(\mathbf{x})$ near a discontinuity, the local polynomial degree p_j is also reduced by one if the approximation is not local extremum conserving (LEC), i.e. if it does not hold that

$$\min_{\mathbf{x} \in T_j} g_j(\mathbf{x}) = \min_{\mathbf{x}_i \in T_j} f(\mathbf{x}_i) \quad \wedge \quad \max_{\mathbf{x} \in T_j} g_j(\mathbf{x}) = \max_{\mathbf{x}_i \in T_j} f(\mathbf{x}_i). \quad (1)$$

Note that the polynomial degree will be at least one. This holds because the linear interpolation problem on a simplex is always uniquely solvable and the resulting interpolation is always local extremum conserving. Since the approximation in one single simplex is independent from all other simplices, the resulting global approximation is not even continuous across the simplices' facets, except for linear polynomials.

2.1.1 The Theoretical Convergence Rate

For smooth functions $f \in \mathcal{C}^{p+1}$ and uniformly distributed sampling points we can locally estimate the approximation error. Let $\{\mathbf{x}_\alpha\}_{|\alpha| \leq p}$ denote the interpolation points with

multi-index $\alpha = (\alpha_1, \alpha_2, \dots, \alpha_d) \in \mathbb{N}_0^d$. The classic estimation [17] for the error in the d -dimensional point $\mathbf{x} = (x^{(1)}, \dots, x^{(d)})$ between the function $f(\mathbf{x})$ and its Lagrange interpolation $L_p f(\mathbf{x})$ of degree p reads

$$|L_p f(\mathbf{x}) - f(\mathbf{x})| \leq \sum_{|\alpha|=p+1} \frac{1}{\alpha!} \left\| \frac{\partial^{p+1} f}{\partial \mathbf{x}^\alpha} \right\|_\infty \prod_{\gamma_1=1}^{\alpha_1} (x^{(1)} - x_{(\gamma_1-1, \alpha_2, \dots, \alpha_d)}^{(1)}) \cdots \prod_{\gamma_d=1}^{\alpha_d} (x^{(d)} - x_{(\alpha_1, \alpha_2, \dots, \gamma_d-1)}^{(d)}). \quad (2)$$

In the i -th product the i -th entry of α is replaced by $\gamma_i - 1$. For n uniformly distributed random points in Ω the expected distance between two of them is of order $\mathcal{O}(n^{-1/d})$. Because each summand consists of $p+1$ factors, each summand is of order $\mathcal{O}(n^{-(p+1)/d})$. Thereby we can estimate the products in (2) and obtain

$$|L_p f(\mathbf{x}) - f(\mathbf{x})| \leq C \cdot n^{-(p+1)/d} \sum_{|\alpha|=p+1} \frac{1}{\alpha!} \left\| \frac{\partial^{p+1} f}{\partial \mathbf{x}^\alpha} \right\|_\infty. \quad (3)$$

Thus the Lagrange interpolation $L_p f$ converges pointwise with order $(p+1)/d$ against the function f if the partial derivatives are bounded. Because the order of convergence depends on the dimension we need to increase the polynomial degree with increasing dimension to obtain a constant order of convergence. The error estimate (3) holds true for any simplex T_j and corresponding approximation $g_j(\mathbf{x})$. Note that for functions $f \in \mathcal{C}^0(\Omega)$ with kinks, i.e. functions that are continuous but not continuously differentiable, we cannot estimate the error with (3) or expect an order of convergence of $(p+1)/d$, as $f \notin \mathcal{C}^{p+1}(\Omega)$. This motivates the following modification of the original approach.

2.2 The Improved SSC

Let $f \in \mathcal{C}^0(\Omega)$ be a function with kinks. We say a function $f : [0, 1]^d \rightarrow \mathbb{R}$ has a kink at the $(d-1)$ -dimensional hyper-surface $K \subset \Omega$ if for all $\mathbf{x} \in K$ the function $f(\mathbf{x})$ is not continuously differentiable. In $d = 2$ dimensions, the kink locations are lines and can be arbitrarily shaped, they can be straight, curved or closed lines, and they can also intersect. In $d = 3$ dimensions, the kink locations are surfaces. We applied the approaches from [20, 21, 22] to functions with kinks, but were not able to reach the desired convergence rates, as can be seen in our numerical experiments in sections 2.4 and 3. Therefore, we developed an improved SSC, which we introduce in the following.

Generally, kinks divide the parameter space Ω into disjoint subdomains Ω_k with $\bigcup_k \Omega_k = \Omega$. Suppose $f \in \mathcal{C}^{p+1}(\Omega_k)$ is smooth for all k , and that we have for each sampling point \mathbf{x}_i the information to which Ω_k it belongs. The last assumption is motivated by our application of gas networks, where one knows if a regulator is active or not, which influences the locations of kinks. There are two different cases for our modification:

Case 1. The function $f(\mathbf{x})$ is smooth in simplices T_j completely contained in some subdomain Ω_k , that is there exists a k with $T_j \subset \Omega_k$. In this case we only search for the nearest neighbor stencil in the reduced set $\{\mathbf{x}_i | \mathbf{x}_i \in \Omega_k\}$, but not in the complete set of sampling points $\{\mathbf{x}_i\}$. As in the original approach, we ensure that the vertices \mathbf{x}_{i_j} of simplex T_j are contained in the nearest neighbor stencil S_j . Since $S_j \subset \Omega_k$, we can approximate a smooth function by polynomial interpolation with known order of convergence $(p_j+1)/d$. Figure 2a shows the improved stencil for a simplex T_j without any kinks inside.

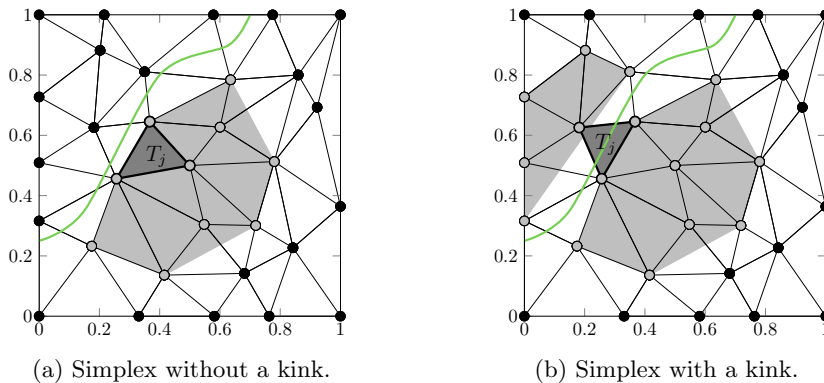


Figure 2: The improved nearest-neighbor stencils (light gray) for simplex T_j (dark gray). The domain Ω is divided by a kink (green) into two subdomains Ω_1 (left) and Ω_2 (right). (a) shown is a stencil for a simplex without a kink inside and completely lying in Ω_2 . (b) shown are two stencils for a simplex with a kink inside and lying in Ω_1 as well as in Ω_2 .

Case 2. Suppose simplex T_j is divided by a kink, that is some of its vertices \mathbf{x}_{i_j} belong to Ω_{j_1} and some to Ω_{j_2} , see Figure 2b. In this case, we search for two nearest neighbor stencils $S_{j,1} \subset \Omega_{j_1}$, $S_{j,2} \subset \Omega_{j_2}$ and two approximations $g_{j,1}(\mathbf{x})$, $g_{j,2}(\mathbf{x})$, one at each side of the kink. As above we ensure that each stencil contains the corresponding vertices \mathbf{x}_{i_j} of T_j . Without loss of generality, we assume that the kink can be represented for all $\mathbf{x}_i \in S_{j,1} \cup S_{j,2}$ as the maximum of both interpolations, i.e.

$$f(\mathbf{x}_i) = \max(g_{j,1}(\mathbf{x}_i), g_{j,2}(\mathbf{x}_i)).$$

Then we extrapolate $g_{j,1}(\mathbf{x})$ and $g_{j,2}(\mathbf{x})$ to simplex T_j and approximate $f(\mathbf{x})$ for all $\mathbf{x} \in T_j$ by taking the maximum of both approximations

$$f(\mathbf{x}) \approx g_j(\mathbf{x}) := \max(g_{j,1}(\mathbf{x}), g_{j,2}(\mathbf{x}))$$

whereby we obtain an approximation to the kink. Figure 3 shows a linear and a quadratic approximation to a kink in simplex T_j . On both stencils S_{j_1} and S_{j_2} the function f is smooth. Both approximations $g_{j,1}(\mathbf{x})$ and $g_{j,2}(\mathbf{x})$ converge with an order of $(p_j + 1)/d$, respectively. Hence, the approximation $g_j(\mathbf{x})$ converges with the same order. Note that this holds also true if $g_{j,1}(\mathbf{x})$ and $g_{j,2}(\mathbf{x})$ do not intersect in T_j . Even if there was not any kink in the function, this procedure of computing two approximations and taking the maximum would not affect the convergence. This is important because in our application an activated regulator, may cause a kink in the flux in some pipes but not in all.

Observe that with this new approach we do not need to fulfill the LEC condition (1) anymore. Since we approximate only smooth functions, no oscillations caused by jumps (Gibb's phenomenon) will arise. Any oscillations due to Runge's phenomenon will result in a larger error estimator and thus in a finer discretization. Indeed, using the LEC limiter would reduce the convergence rate if there are some small oscillations in $f(\mathbf{x})$.

2.3 Refinement Strategies

While it is possible to construct an approximation for a given set of sampling points, we want to start with an initial set of sampling points consisting of the corners and the center

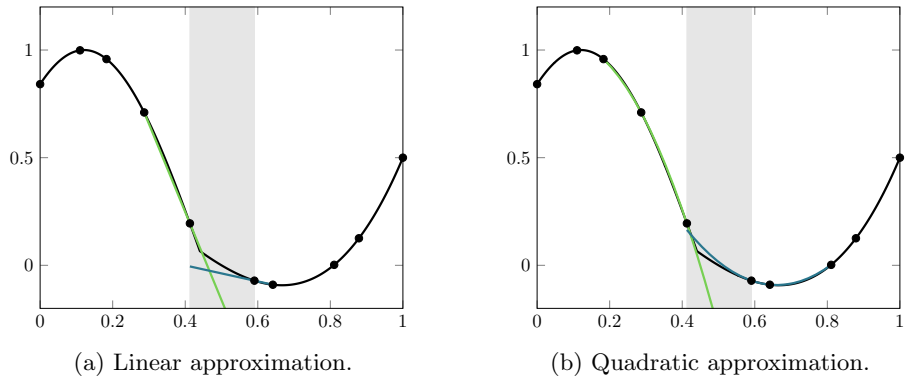


Figure 3: A linear (a) and quadratic (b) approximation of a kink, each with two stencils. The function $f(x)$ is colored in black, the left hand approximation $g_{j,1}(x)$ in green and the right hand approximation $g_{j,2}(x)$ in blue.

of Ω . To adaptively refine the discretization we then successively add new points at those simplices for which a to be defined error estimator is the largest. In the end we aim for less points in regions where $f(\mathbf{x})$ is flat and more points in regions where $f(\mathbf{x})$ varies more. For an adaptive refinement we need on the one hand a strategy of how to add new points and on the other hand a reliable error estimator.

2.3.1 Adding a New Sampling Point

In [21] simplex T_j is refined by sampling a new random point in a subsimplex T_{sub_j} . The vertices $\mathbf{x}_{\text{sub}_j,l}$ are defined as the centers of the faces of simplex T_j

$$\mathbf{x}_{\text{sub}_j,l} = \frac{1}{d} \sum_{\substack{l^*=0 \\ l^* \neq l}}^d \mathbf{x}_{i_j,l^*}.$$

See Appendix A.1 for an efficient way to sample random points from a uniform distribution over some simplex. Figure 4a shows the subsimplex T_{sub_j} of simplex T_j . This sampling strategy results in long and flat simplices at the boundary because the new sampling point will almost surely not be added at the boundary. Therefore, we use this strategy only for simplices without a facet at the boundary. Simplices with a facet at the boundary are refined by adding a new sampling point on the middle third of the longest edge, as introduced in [20]. Let $\mathbf{x}_{i_j,0}$ and $\mathbf{x}_{i_j,1}$ be the endpoints of the longest edge of simplex T_j , then we define the new sampling point $\mathbf{x}_{i_{\text{new}}}$ as

$$\mathbf{x}_{i_{\text{new}}} = \mathbf{x}_{i_j,0} + \frac{1+u}{3} (\mathbf{x}_{i_j,1} - \mathbf{x}_{i_j,0}),$$

where u is a uniformly distributed random variable in $[0, 1]$. Figure 4b shows the sampling area on the longest edge of a boundary simplex T_j .

2.3.2 Error Estimation

To refine the simplex with the largest error we need an error estimator since we cannot compute the exact error. First, we introduce two newly developed solution-based error estimators and then a third already existing error estimator that does not directly depend

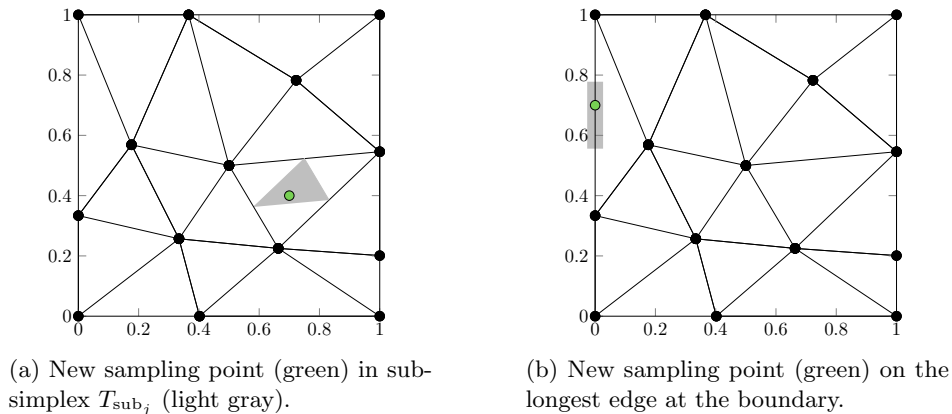


Figure 4: Shown are different refinement strategies for simplices with all facets lying in the interior of the domain Ω (a) and for simplices with a facet lying at the boundary $\partial\Omega$ (b).

on the solution. The third one is very useful when the function $f(\mathbf{x})$ has more than one output.

Error Estimation Based on a Single Point. In [20] a solution-based error estimator ε_j is proposed where the square of the hierarchical error $\epsilon_{i_{\text{new},j}} = |f(\mathbf{x}_{i_{\text{new},j}}) - g_j(\mathbf{x}_{i_{\text{new},j}})|$ between approximation and function at the new sampling point $\mathbf{x}_{i_{\text{new},j}}$ is weighted with the volume of the simplex

$$\varepsilon_j = \text{vol}(T_j) \cdot \epsilon_{i_{\text{new},j}}^2. \quad (4)$$

This error estimator has the disadvantage that we need to evaluate the function f at point $\mathbf{x}_{i_{\text{new},j}}$, although the point might not be added to the discretization. To avoid these useless function evaluations we modify the original error estimator. We do not use the hierarchical error in the new sampling point $\mathbf{x}_{i_{\text{new},j}}$, but instead in the last added sampling point of simplex T_j before adding it. Let $i_{j^*} = \max_l i_{j,l}$ be the index of this last added sampling point and T_{ref,j^*} the simplex which was refined by adding $\mathbf{x}_{i_{j^*}}$. Then, the hierarchical error is given by

$$\epsilon_{i_{j^*}} = |f(\mathbf{x}_{i_{j^*}}) - g_{\text{ref},j^*}(\mathbf{x}_{i_{j^*}})|$$

and we obtain the error estimator

$$\tilde{\varepsilon}_j = \text{vol}(T_j) \cdot \epsilon_{i_{j^*}}^2.$$

By summing up the error estimators for all simplices $\{T_j\}$ we can approximate the root mean square error in Ω by

$$\tilde{\varepsilon}_{\text{rms}} = \sqrt{\sum_{j=1}^m \tilde{\varepsilon}_j} = \sqrt{\sum_{j=1}^m \text{vol}(T_j) \cdot \epsilon_{i_{j^*}}^2}.$$

Error Estimation Based on Monte Carlo Integration. Because we do not want to rely on the error in one single point, we develop a new error estimator. It is an approximation

of the L_1 error between $g_j(\mathbf{x})$ and the function $f(\mathbf{x})$ in a given simplex T_j . For this, we approximate $\varepsilon_j = \|f - g_j\|_{L_1(T_j)}$ by Monte Carlo integration, i.e.

$$\varepsilon_j \approx \text{vol}(T_j) \sum_{i=1}^{n_{\text{MC}}} \frac{|f(\mathbf{x}_{\text{MC},i}) - g_j(\mathbf{x}_{\text{MC},i})|}{n_{\text{MC}}} \quad (5)$$

at n_{MC} randomly drawn Monte Carlo points $\mathbf{x}_{\text{MC},i}$. It is not feasible to evaluate f at all n_{MC} Monte Carlo points because each function evaluation can be an expensive simulation. Thus we approximate the right hand side of (5) with the polynomial interpolation \bar{g}_j in stencil S_j of degree $p_j - 1$. We define

$$\hat{\varepsilon}_j = \text{vol}(T_j) \sum_{i=1}^{n_{\text{MC}}} \frac{|g_j(\mathbf{x}_{\text{MC},i}) - \bar{g}_j(\mathbf{x}_{\text{MC},i})|^{(p_j+1)/p_j}}{n_{\text{MC}}}.$$

The exponent $(p_j + 1)/p_j$ is necessary since the approximation with \bar{g}_j only leads to an order of convergence of p_j/d , whereas the approximation g_j converges with order $(p_j + 1)/d$. Thereby we ensure that the error estimator decreases with the same rate as the true error. If $p_j = 1$, we define the constant function \bar{g}_j as $\bar{g}_j(\mathbf{x}) = \min_{i_j} f(\mathbf{x}_{i_j})$. To obtain an overall error estimation, we sum up the error estimators for all simplices $\{T_j\}$

$$\hat{\varepsilon}_{l_1} = \sum_{j=1}^m \hat{\varepsilon}_j.$$

Error Estimation Based on the Theoretical Order of Convergence. If one has a function $f(\mathbf{x})$ with a multidimensional output, a solution-based error estimator could not be used because one usually does not know how the error scales over different outputs. Therefore we use a solution-independent error estimator, as described in [20]. For this consider the definition of the order of convergence

$$\mathcal{O} = \frac{\log(\varepsilon_0/\varepsilon_j)}{\log(\text{vol}(\Omega)/\text{vol}(\Omega_j))}$$

for some reference error ε_0 . Then the error ε_j in simplex T_j is proportional to

$$\varepsilon_j \sim \text{vol}(T_j)^{\mathcal{O}} = \text{vol}(T_j)^{(p_j+1)/d}.$$

Weighting this again with the volume of simplex T_j yields the error estimator

$$\bar{\varepsilon}_j = \text{vol}(T_j) \cdot \varepsilon_j = \text{vol}(T_j)^{(p_j+1)/d+1}.$$

It only depends on the volume of simplex T_j and the theoretical order of convergence $\mathcal{O} = (p_j + 1)/d$. For an overall error estimator we sum again over all simplices

$$\bar{\varepsilon}_{\mathcal{O}} = \sum_{j=1}^m \bar{\varepsilon}_j.$$

2.4 Numerical Results for Test Functions

Here, we provide numerical results for smooth and non-smooth functions. To verify the convergence rates we calculate the approximation error as the l_1 norm between $f(\mathbf{x})$ and $g(\mathbf{x})$ evaluated at $n_{\text{MC}} = 10^6$ uniformly in Ω distributed Monte Carlo points:

$$\varepsilon_{l_1} = \sum_{i=1}^{n_{\text{MC}}} \frac{|f(\mathbf{x}_{\text{MC},i}) - g(\mathbf{x}_{\text{MC},i})|}{n_{\text{MC}}}.$$

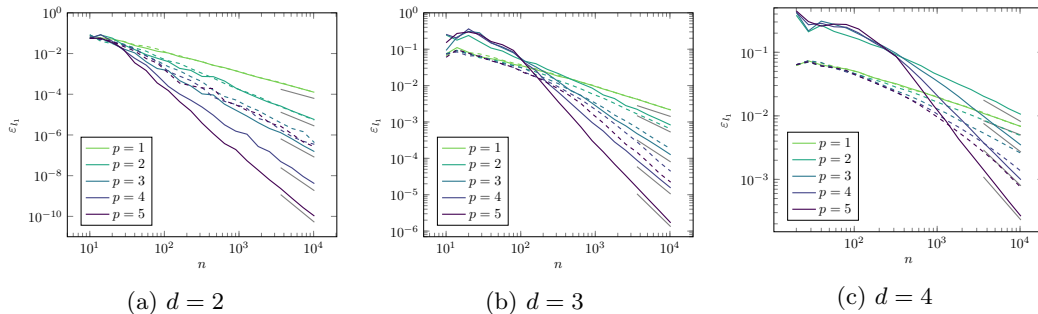


Figure 5: Shown is the l_1 error evaluated at 10^6 random points versus the number n of sampling points for the smooth test function in $d = 2, 3, 4$ dimensions with (dashed lines) and without (solid lines) the LEC condition. The theoretical convergence rates are colored in gray.

2.4.1 Smooth Functions

First we evaluate the simplex stochastic collocation algorithm with some smooth function $f \in C^\infty([0, 1]^d)$

$$f(\mathbf{x}) = \prod_{i=1}^d \sin(\pi x^{(i)}),$$

for the Monte Carlo based error estimator $\hat{\epsilon}_j$ with and without the local extremum conserving condition. In Figure 5 we see that the algorithm without the LEC condition yields slightly better results for $d \leq 3$. Since the function is smooth, oscillations due to kinks or jumps cannot occur. Enforcing the local extremum conservation decreases the polynomial degree p_j if the function $f(\mathbf{x})$ itself has some small oscillations in simplex T_j . This reduction of the polynomial degree is not necessary and impairs convergence.

But, with increasing dimension we benefit from using the condition of local extremum conservation in the pre-asymptotic behavior. Therefore, we will use a weaker formulation of the local extremum conserving condition for dimensions $d \geq 4$ in the following. We will only reduce the polynomial degree of the approximation by one, if it does not hold that

$$\min_{\mathbf{x} \in T_j} g_j(\mathbf{x}) + \delta \geq \min_{\mathbf{x}_i \in T_j} f(\mathbf{x}_i) \quad \wedge \quad \max_{\mathbf{x} \in T_j} g_j(\mathbf{x}) - \delta \leq \max_{\mathbf{x}_i \in T_j} f(\mathbf{x}_i),$$

with $\delta = 0.5(\max_{\mathbf{x}_i \in T_j} f(\mathbf{x}_i) - \min_{\mathbf{x}_i \in T_j} f(\mathbf{x}_i))$. This δ -local extremum conserving (δ -LEC) condition allows small oscillations in the approximation and improves the pre-asymptotic behavior without affecting the convergence. See Figure 6c for the error in $d = 4$ dimensions with this weaker condition.

Above we stated that calculating two approximations on both sides of an assumed kink does not affect the convergence rate if in fact there is no kink. In order to verify this, we took the same test function $f(\mathbf{x}) = \prod_{i=1}^d \sin(\pi x_i)$ and assumed a kink at $f(\mathbf{x}) = 0.7$. That is, we check if the function value $f(\mathbf{x}_i)$ is smaller or equal to 0.7, so we can assign each sampling point x_i either to $\Omega_1 = \{\mathbf{x} \in \Omega : f(\mathbf{x}) < 0.7\}$ or to $\Omega_2 = \{\mathbf{x} \in \Omega : f(\mathbf{x}) = 0.7\}$. This replicates the effect of a regulator in a gas network. See Figure 6 for the results. Assuming a kink yields slightly larger errors, but in all cases the desired convergence rates are attained. The difference between assuming and not assuming a kink decreases with increasing number n of sampling points. Note that for $d = 4$ dimensions we have already used the δ -local extremum conservation.

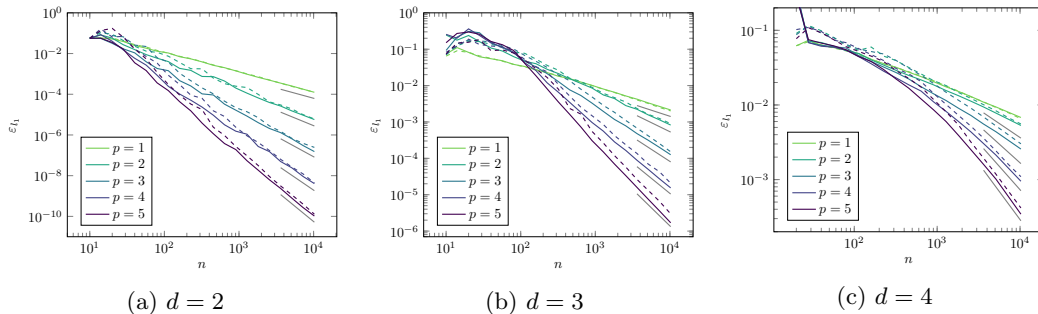


Figure 6: Shown is the l_1 error evaluated at 10^6 random points versus the number n of sampling points for the smooth test function in $d = 2, 3, 4$ dimensions with (dashed lines) and without (solid lines) the assumption of a kink at $f(\mathbf{x}) = 0.7$. The theoretical convergence rates are colored in gray. Dimensions $d = 2$ and $d = 3$ are without the LEC condition and $d = 4$ is with the δ -LEC condition.

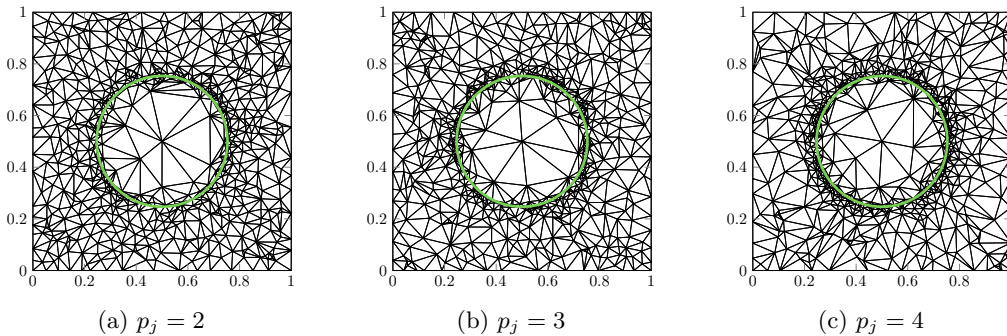


Figure 7: Original SSC: Shown is an adaptively refined Delaunay triangulation of $n = 640$ sampling points for the non-smooth test function with different polynomial degrees of $p_j = 2, 3, 4$ and the l_1 error estimator $\tilde{\varepsilon}_j$. The location of the kink is marked in green.

2.4.2 Non-Smooth Functions

Consider the test function

$$f(\mathbf{x}) = \min \left(\prod_{i=1}^d \sin(\pi x^{(i)}), 0.7 \right).$$

First we show numerical results for the original simplex stochastic collocation version [21] with the local extremum conservation and no special approximation for kinks. As expected, enforcing the local extremum conservation reduces the polynomial degree near the kink, which results in a larger error estimator and thus in a finer discretization, see Figure 7. The higher the polynomial degree is, the more points are added near the kink. We expected this behavior because the smooth part of f can be better approximated with polynomials of higher degree, whereas increasing the degree of the interpolating polynomials does not benefit approximating the kink.

See Figure 8 for the convergence rates of the original simplex stochastic collocation with the original error estimator ε_j . In $d = 2$ dimensions, the desired convergence rates are attained for small polynomial degrees $p = 1$ and $p = 2$. Increasing the polynomial degrees up

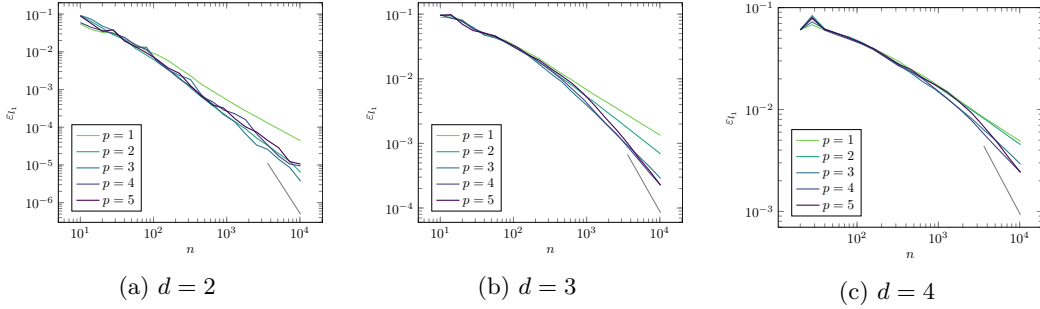


Figure 8: Original SSC: Shown is the l_1 error evaluated at 10^6 random points versus the number n of sampling points for different dimensions $d = 2, 3, 4$ with the l_1 error estimator $\tilde{\varepsilon}_j$. The desired convergence rates for a polynomial degree of $p = 5$ are plotted in gray.

to $p = 3$, $p = 4$ and $p = 5$ does not improve the convergence rate and hence the theoretical orders of 2, 2.5 and 3 are not attained. In $d = 3$ dimensions the errors for $p = 3$, $p = 4$ and $p = 5$ are nearly the same with a maximal order of 1.3 instead of 2. For dimensions larger or equal to $d = 4$ using polynomials of higher degree is not beneficial and the maximally attained order of convergence is 0.75. Therefore, the original simplex stochastic collocation is useless for computing statistics of the solution in $d \geq 4$ dimensions. For these cases Monte Carlo methods provide comparable results with less computational effort.

Now we analyze the modified simplex stochastic collocation method. As before, we check if the function value is smaller or equal to 0.7 to simulate a regulator in a gas network. An adaptively refined Delaunay triangulation obtained with the l_1 error estimator $\hat{\varepsilon}_j$ for $p_j = 5$ and $n = 640$ sampling points can be found in Figure 9a. As expected, the sampling points are more or less uniformly distributed over the parameter space Ω where the function value is not constant. In the center of our domain where the function value is constant, the areas of the triangles are significantly larger. The triangulation in Figure 9b, using the root mean square error estimator $\tilde{\varepsilon}_j$, looks quite similar: there are fewer triangles in the center than around it where the triangles are less uniformly sized as for the estimator $\hat{\varepsilon}_j$. In contrast, the triangulation resulting from the function-independent error estimator $\bar{\varepsilon}_j$ is uniform. It is not possible to recognize the location of the kink, see Figure 9c.

In all shown dimensions $d = 2, 3, 4$ nearly all theoretical convergence rates of ε_{l_1} evaluated at $n_{MC} = 10^6$ Monte Carlo points are attained for the l_1 error estimator as well as for the root mean square error estimator $\hat{\varepsilon}_j$, and the error estimator $\bar{\varepsilon}_j$, cf. Figure 10. The l_1 error estimator yields the best results and the smoothest convergence. The pointwise error estimator $\tilde{\varepsilon}_j$ yields comparable results and both error estimators can be used as a reliable stopping criterion. The total errors reached with error estimator $\bar{\varepsilon}_j$ in $d = 2$ and $d = 3$ dimensions look quite similar, but as expected the estimated overall error differs greatly from the real error because it is not solution-based. So this error estimator should not be used as stopping criterion. Moreover, this is also the reason for the worse results in $d = 4$ dimensions. The error estimator $\bar{\varepsilon}_j$ overestimates the real error in simplices where the polynomial degree has been reduced for fulfilling the δ -LEC condition. Omitting the δ -LEC condition in this case would decrease the error for a large number of sampling points but at the expense of a worse pre-asymptotic. Comparing these total errors with those obtained with the original simplex stochastic collocation method and the original pointwise error estimator ε_j , shows that the modification yields significantly better results. The total error

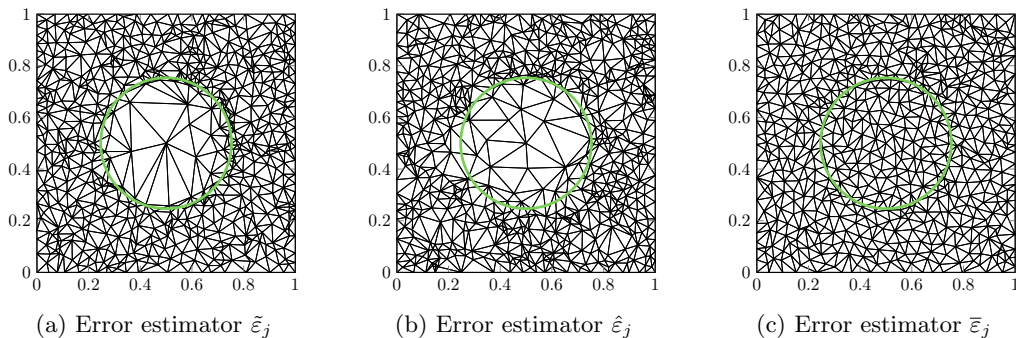


Figure 9: Modified SSC: Shown is an adaptively refined Delaunay triangulation with $n = 640$ sampling points for the function $f(\mathbf{x}) = \min(\prod_{i=1}^d \sin(\pi x^{(i)}), 0.7)$ in 2d with a polynomial degree of $p_j = 5$ for the l_1 error estimator $\tilde{\epsilon}_j$ (a), for the root mean square error estimator $\hat{\epsilon}_j$ (b), and for the function-independent error estimator $\bar{\epsilon}_j$ (c). The location of the kink is marked in green.

for the maximal number of points was improved from $3 \cdot 10^{-6}$ to $4 \cdot 10^{-11}$ in two dimensions, from $2 \cdot 10^{-4}$ to $2 \cdot 10^{-6}$ in three dimensions, and from $2 \cdot 10^{-3}$ to $3 \cdot 10^{-4}$ in four dimensions.

2.4.3 Multiple Refinements

In order to parallelize the refinement, at each step the $m_{\text{ref}} \geq 1$ simplices with the largest error estimator can be refined. Thus, the function evaluations for the new sampling points can be done simultaneously and the expensive update of the Delaunay triangulation needs just to be done once instead of m_{ref} times. Figure 11 shows the three error estimators versus the percentage of simplices. The results are comparable for all dimensions and all error estimators, the only exception is error estimator $\bar{\epsilon}_j$ in $d = 4$ dimensions. In this case, the estimated error in 20 % of the simplices is higher than expected. These are exactly the simplices where the polynomial degree was reduced for fulfilling the δ -LEC condition. In all other cases, the error estimator slowly decreases over most simplices independent of dimension, polynomial degree, and type of error estimator. Only for a small percentage of simplices the error estimator is significantly smaller than for the rest. Thereby it is reasonable to add several sampling points at once.

Figure 12 shows the convergence rates for multiple refinements where we used the Monte Carlo based error estimator $\tilde{\epsilon}_j$ and at each step added $0.3n$, $0.6n$, or $0.9n$ points, respectively, to the current discretization consisting of n sampling points. Since the number of newly added sampling points does not influence the convergence, it is reasonable to refine multiple simplices to save computational time.

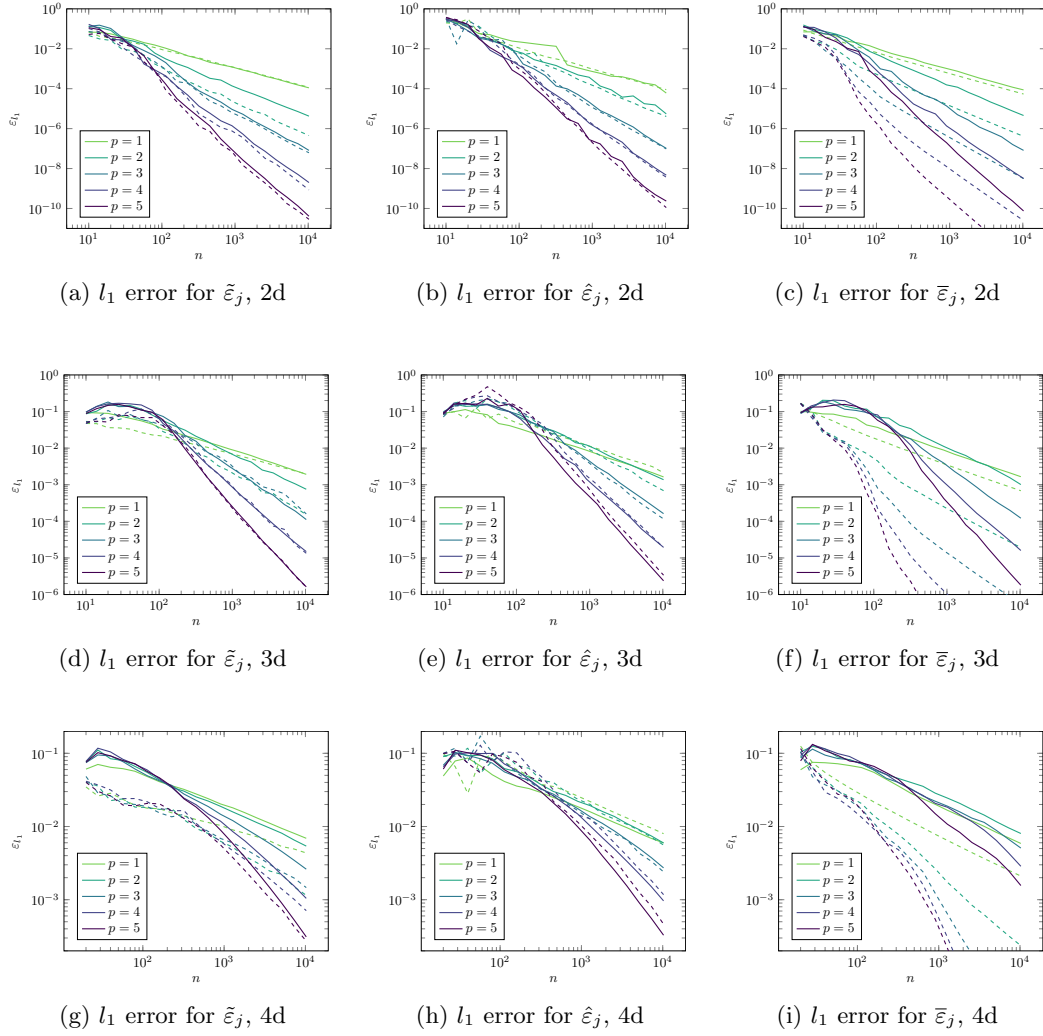


Figure 10: Modified SSC: Shown is the l_1 error evaluated at 10^6 random points (solid) and the error estimator (dashed) versus the number n of interpolation points for the l_1 error estimator $\tilde{\varepsilon}_j$ (a), the root mean square error estimator $\hat{\varepsilon}_j$ (b), and the error estimator $\bar{\varepsilon}_j$ (c).

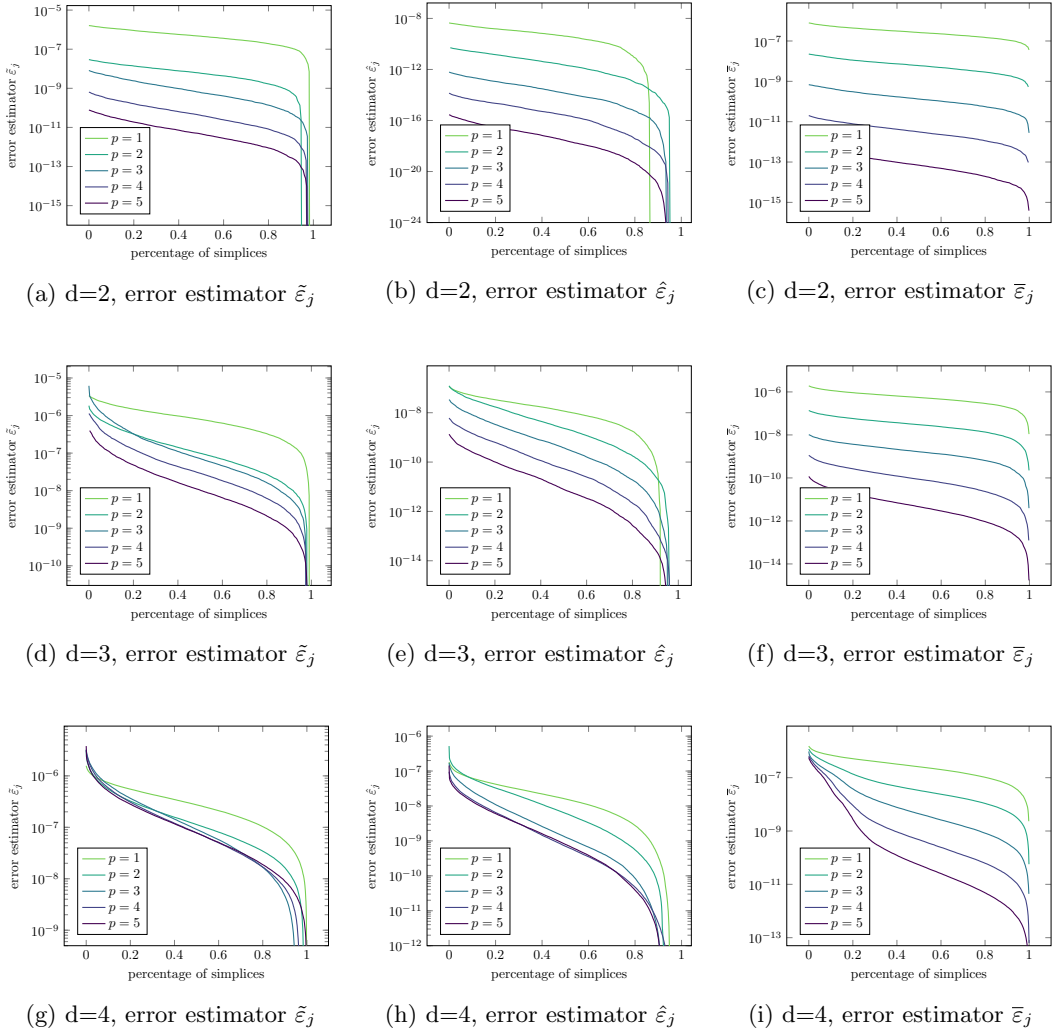


Figure 11: Shown is the distribution of the l_1 error estimator over the percentage of simplices for different error estimators. In all cases, $m = 1000$ sampling points are used for the triangulation.

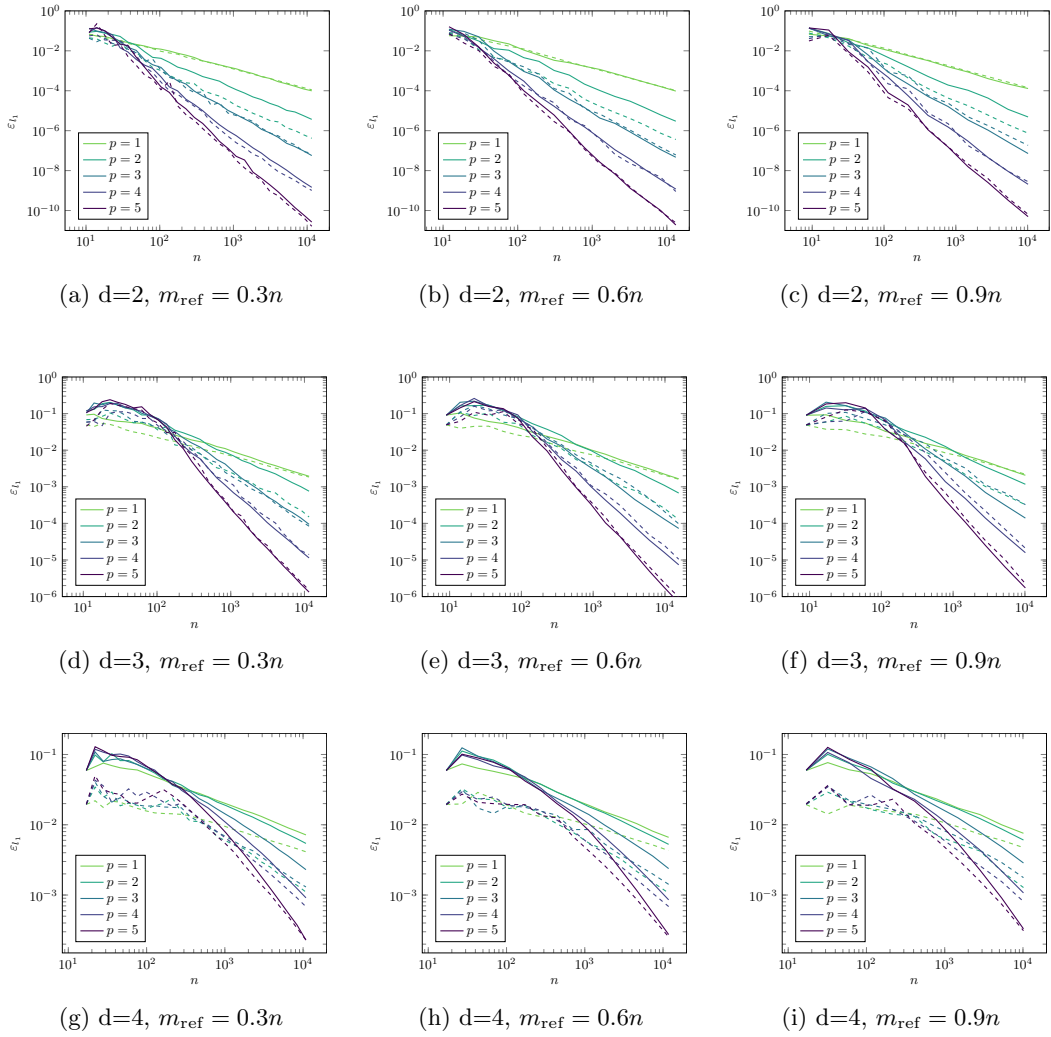


Figure 12: Shown is the l_1 error evaluated at 10^6 random points (solid) and the error estimator (dashed) versus interpolation points n for l_1 error estimator $\tilde{\varepsilon}_j$. At each refinement step 30% (left column), 60% (central column), and 90% (right column) of the old sampling points were added.

2.5 Statistics of the Approximated Function

When simulating gas networks some input data can be uncertain like the pressure of the injected gas at input nodes or the flux of the extracted gas at demand nodes. The response of the gas network to these uncertainties are expressed by the pressure and temperature at nodes and the flux through pipes. We are interested in statistics of these physical quantities like the expected value, variance, or median. The cumulative density function (cdf) can be used to determine the probability that a production-related critical value, for example the maximum pressure a pipe can withstand, will be exceeded.

Expectation. The expectation of a function $f(\mathbf{x})$ of a random variable $\mathbf{x} \in \Omega$ with the density function $\rho(\mathbf{x})$ can be approximated by using the approximations $g_j(\mathbf{x})$ on the simplices T_j in the evaluation of a quadrature rule Q for the approximation \tilde{f} of f , i.e.

$$\mathbb{E}[f] = \int_{\Omega} f(\mathbf{x})\rho(\mathbf{x}) \, d\mathbf{x} \approx Q(\tilde{f}) = \sum_{j=1}^m Q(g_j).$$

The quadrature rule Q can be a Monte Carlo integration or a Gaussian quadrature, where we do not evaluate f for any quadrature point, but only the approximations g_j , which are cheap to evaluate.

Variance. The variance of a function $f(\mathbf{x})$ of a random variable $\mathbf{x} \in \Omega$ with the density function $\rho(\mathbf{x})$ is defined as the squared distance of the function from its mean. We approximate the variance in the same way as the expectation, namely by using Monte Carlo integration or Gaussian quadrature to calculate the integrals, i.e.

$$\mathbb{V}[f] = \int_{\Omega} (f(\mathbf{x}) - \mathbb{E}[f])^2 \rho(\mathbf{x}) \, d\mathbf{x} = \mathbb{E}[f^2] - \mathbb{E}[f]^2 \approx Q(\tilde{f}^2) - Q(\tilde{f})^2.$$

Convergence. The absolute error of the expectation $|\mathbb{E}[f] - Q(\tilde{f})|$ can be estimated as

$$\begin{aligned} |\mathbb{E}[f] - Q(\tilde{f})| &\leq \left| \mathbb{E}[f] - \mathbb{E}[\tilde{f}] \right| + \left| \mathbb{E}[\tilde{f}] - Q(\tilde{f}) \right| \\ &\leq \int_{\Omega} |f(\mathbf{x}) - \tilde{f}(\mathbf{x})| \rho(\mathbf{x}) \, d\mathbf{x} + \left| \mathbb{E}[\tilde{f}] - Q(\tilde{f}) \right| \\ &\leq \int_{\Omega} \underbrace{|f(\mathbf{x}) - \tilde{f}(\mathbf{x})|}_{\varepsilon_I(f)} \rho(\mathbf{x}) \, d\mathbf{x} + \underbrace{\left| \mathbb{E}[\tilde{f}] - Q(\tilde{f}) \right|}_{\varepsilon_Q(f)} \\ &= \varepsilon_I(f) + \varepsilon_Q(f). \end{aligned}$$

The interpolation error $\varepsilon_I(f)$ can be estimated by (3). If we choose the quadrature formula such that the quadrature error $\varepsilon_Q(f)$ is at most of the same order of magnitude as the interpolation error $\varepsilon_I(f)$, then the approximation $Q(\tilde{f})$ of the expected value $\mathbb{E}[f]$ converges also with an order of $(p+1)/d$, provided that the partial derivatives are bounded.

The same rate can be obtained for the variance, if the function and all partial derivatives are bounded. Using the triangle inequality we get the following two terms:

$$\left| \mathbb{V}[f] - (Q(\tilde{f}^2) - Q(\tilde{f})^2) \right| \leq \left| \mathbb{E}[f^2] - Q(\tilde{f}^2) \right| + \left| \mathbb{E}[f]^2 - Q(\tilde{f})^2 \right|. \quad (6)$$

Analogously to the expectation, the first term can be estimated by

$$\left| \mathbb{E}[f^2] - Q(\tilde{f}^2) \right| \leq \varepsilon_I(f^2) + \varepsilon_Q(f^2).$$

With $|f^2 - \tilde{f}^2| \leq |f - \tilde{f}| |f + \tilde{f}| \leq |f - \tilde{f}| (|f| + |\tilde{f}|)$ we obtain

$$\left| \mathbb{E}[f^2] - Q(\tilde{f}^2) \right| \leq (|f| + |\tilde{f}|) \varepsilon_I(f) + \varepsilon_Q(f^2).$$

Next we consider the second term of (6):

$$\begin{aligned} \left| \mathbb{E}[f]^2 - Q(\tilde{f})^2 \right| &\leq \left| \mathbb{E}[f] - Q(\tilde{f}) \right| \left(|\mathbb{E}[f]| + |Q(\tilde{f})| \right) \\ &\leq (\varepsilon_I(f) + \varepsilon_Q(f)) \left(|\mathbb{E}[f]| + |Q(\tilde{f})| \right). \end{aligned}$$

Assuming bounded $f, \tilde{f}, \mathbb{E}[f], Q(\tilde{f}) \leq C$, we get the following result for the error of the variance

$$\begin{aligned} \left| \mathbb{V}[f] - (Q(\tilde{f}^2) - Q(\tilde{f})^2) \right| &\leq 2C \varepsilon_I(f) + \varepsilon_Q(f^2) + 2C \varepsilon_I(f) + 2C \varepsilon_Q(f) \\ &\leq 4C \varepsilon_I(f) + 2C \varepsilon_Q(f) + \varepsilon_Q(f^2). \end{aligned}$$

Hence, by choosing the quadrature formula such that the quadrature errors $\varepsilon_Q(f)$ and $\varepsilon_Q(f^2)$ are at most of the same order of magnitude as the interpolation error $\varepsilon_I(f)$, yields again an order of convergence of $(p+1)/d$.

CDF. For approximating the cumulative density function $\mathbb{P}[f(\mathbf{x}) \leq y]$, we discretize the value range of the approximation g with equidistant nodes y_0, y_1, \dots, y_n where $y_i = \min(g) + ih$ and $h = (\max(g) - \min(g))/n$. For each node y_i we determine the maximal domain $\Omega_i \subseteq \Omega$ such that $g(\mathbf{x}) \leq y_i$ for all $\mathbf{x} \in \Omega_i$. With the probabilities of these domains we obtain the function values of the cumulative density function because it holds

$$\mathbb{P}[g(\mathbf{x}) \leq y_i] = \mathbb{P}[\Omega_i].$$

As a last step we interpolate the cumulative density function between the nodes, e.g. with piecewise linear polynomials. Note that the interpolation must be monotonically increasing because otherwise the resulting function does not fulfill the requirements of a cumulative density function.

3 Uncertainty Quantification for Gas Network Simulation

Today, natural gas contributes significantly to many countries energy supply, where it is used to provide heat and power. Additionally natural gas is an input for producing plastics and chemicals in industry. A large number of scenario analyses are necessary to ensure a secure and reliable operation of a gas network. Since usually these scenarios cannot be easily tested, they are replaced by simulations. Uncertainties arise in the withdrawn amount of gas of each customer. For example, it is then of great interest whether the gas network can meet the demand when all customers need a lot of gas at once and how likely a failure is. For this forward propagation we use the method of simplex stochastic collocation to approximate and integrate high-dimensional functions.

3.1 Euler Equations for Pipes

A gas network is modeled with nodes and edges. The edges represent pipes or other network elements such as valves, control valves, heaters, or compressors. Gas flow through a single pipe of length L with diameter A is described by the Euler equations, a set of partial differential equations [9, 10, 18]. The first equation is the continuity equation

$$\partial_t \rho + \partial_x(\rho v) = 0, \quad (7)$$

following from the conservation of mass. The law of momentum conservation

$$\frac{1}{A} \partial_t q + \partial_x(\rho v^2) + g\rho \partial_x h + \partial_x p + \frac{\lambda}{2D} \rho |v|v = 0, \quad (8)$$

specifies the pressure loss along the pipe due to weight, pressure, and frictional forces. The equation of state

$$p = z(p, T) \rho R_s T \quad (9)$$

is necessary to describe the state of a real compressible gas for a given set of values for temperature T , density ρ , and pressure p . The first law of thermodynamics must be taken into account to describe any heat transfer process. A solution to this system of equations can be found analytically if we assume a stationary and isothermal gas flow [18]. Analogously to Kirchhoff's law, the mass must be conserved at junctions where several pipes are connected. At supply nodes the incoming gas pressure is given, whereas at demand nodes the extracted mass flow. If a gas network consists of pipes only, the solution of the pressure, density, and temperature at nodes and the gas flow in pipes is sufficiently smooth. But a real gas network also contains more complicated elements. For an overview over other elements and the corresponding equations see [4]. In that work errors due to model assumptions were investigated, for realistic situations these can be in the order of 10^{-4} .

3.2 Kinks due to pressure regulation

Usually, the pressure in transport pipes is significantly larger than the maximum allowable operating pressure in distributional pipes. Due to this reason the network needs pressure control valves that adjust the outgoing pressure if the incoming pressure exceeds a preset limit. Unfortunately, the more complicated elements impair the smoothness of the solution. For example, a pressure control valve causes kinks in the solution. Increasing the pressure at a supply node increases the pressure after a control valve until the preset pressure is reached, but afterwards the pressure remains constant, see Figure 13. We do not know in advance where the kink is located, but after the simulation run we know if a control valve is active or not. This information is necessary to use our improved simplex stochastic collocation.

In this section we apply our new version of simplex stochastic collocation to a real gas network where we used [1] to simulate the gas flow. The network has one supply node, 37 demand nodes, several pipes, and five control valves which reduce the high pressure of about 27 bar at the supply node stepwise to pressures of around 16, 8, and 4 bar at the demand nodes. See Figure 14 for a schematic drawing of the network. Different pressure levels are shown in different colors. In all tests, the quantity of interest is the outgoing pressure $f(\mathbf{x})$ at the right control valve. Depending on the uncertain parameters of outgoing pressure x_1 at the left valve, and the amount of withdrawn gas at demand nodes x_2 , x_3 , and x_4 , the right valve is in an active or bypass mode. This is checked by comparing the outgoing pressure with the preset pressure. The lower the outgoing pressure x_1 is, and the higher the withdrawn amount of gas is, the lower is the incoming pressure $f(\mathbf{x})$ at the right control valve.

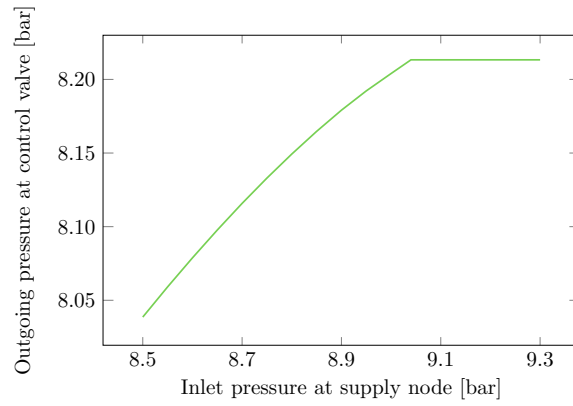


Figure 13: A kink in the solution resulting from pressure regulation.

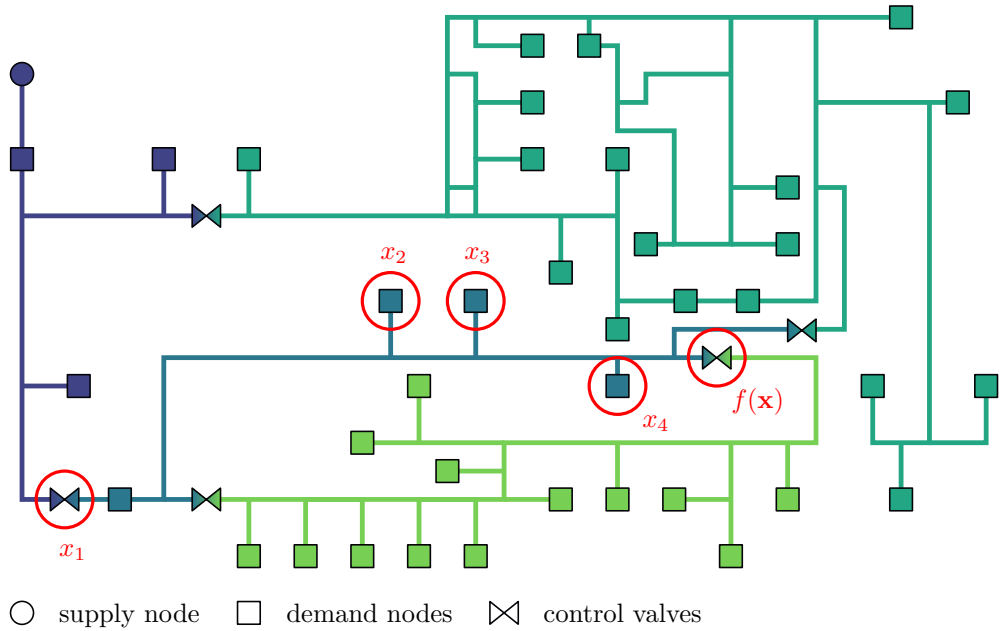


Figure 14: Test gas network with one supply node, 37 demand nodes, and five pressure control valves.

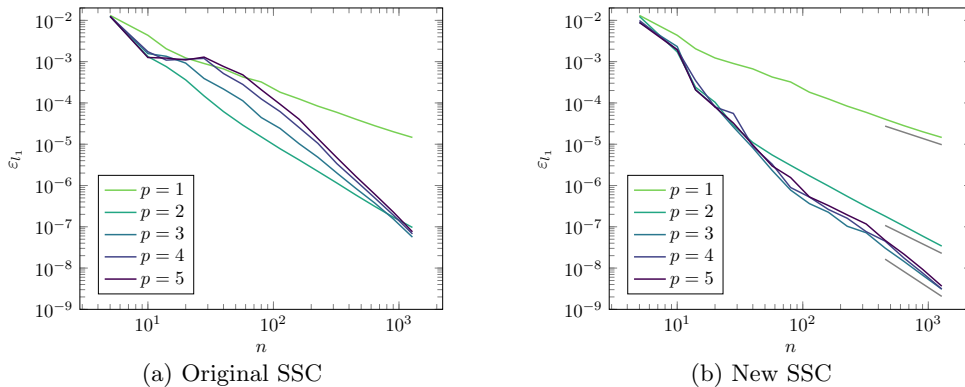


Figure 15: $d = 2$. The l_1 error evaluated at 10^6 random points versus the number n of interpolation points with l_1 error estimator $\tilde{\varepsilon}_j$ for the original SSC without kink information (a), and for the new version with kink information (b).

3.3 Input Uncertainties in Two Dimensions

First, we vary the outgoing pressure x_1 of the left control valve uniformly between 8.5 bar and 9.5 bar, and the demanded power x_2 uniformly between 160 MW and 200 MW. The remaining powers are fixed, in particular $x_3 = 250$ MW and $x_4 = 17$ MW. See Figure 15 for a comparison of the results using the original simplex stochastic collocation (a) with those from our improved one (b). The new version yields better results than the original one, the smallest error reached is two orders of magnitude smaller. In the original version it makes no difference whether polynomials of degree $p = 2$ or higher are used. In the new version the desired convergence rates (marked in gray) for $p = 1$, $p = 2$, and $p = 3$ are obtained. Increasing the polynomial degree to $p = 4$ or $p = 5$ yields no improvement in the rate. Similar results are valid for the expected value, where a reference value was computed with a polynomial degree of $p = 5$ and $m = 5120$ sampling points, see Figure 16. The original simplex stochastic collocation needs $m \approx 50$ sampling points to achieve an accuracy of 10^{-4} , about the order of the model error, whereas the new version only needs $m \approx 30$ sampling points.

The question is why we cannot improve the convergence rate using higher order polynomials as it was the case for the synthetic test function in the previous section? To answer this question see Figure 17. The surface plot of the function (a) is inconspicuous. But if we look at the resulting triangulation (b), we can see that there are two areas in which the error estimator places an unexpected number of points. This indicates discontinuities. Because of this, we approximated the second order partial derivative $\partial_{x_1} f(\mathbf{x})$ with the second order finite difference quotient (c) and, hence, we can see two jumps in the second partial derivative which explain the poor convergence results. After investigation with the developers of the solver MYNTS [1], it can be determined that these jumps are not caused by the physical properties of gas flow but by the specific numerical treatment of the underlying solver to obtain convergence. It is not predictable where these arise, so we do not have a possibility to adapt the method. In principal, these jumps due to the numerical treatment in MYNTS could be avoided, but this would effect the overall solution process and convergence to a solution would not any longer be guaranteed without further measures. Since the employed version of the solver is completely sufficient in its accuracy and behavior for current industrial applications, there is so far no practical need to overhaul it.

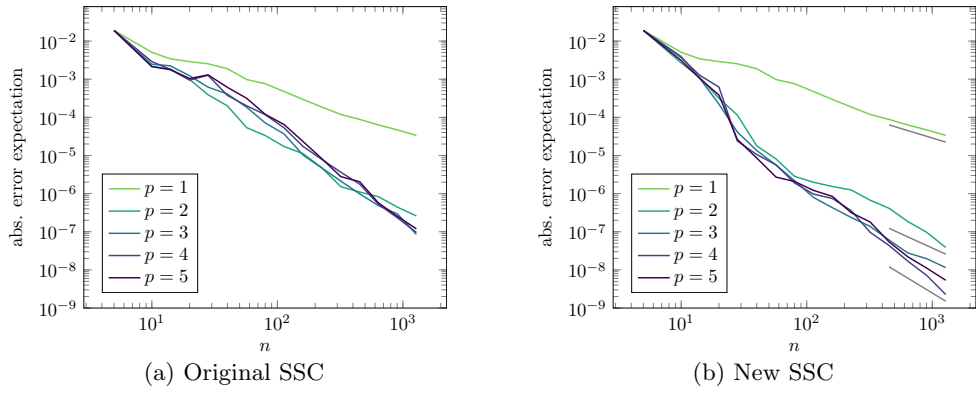


Figure 16: $d = 2$. The absolute error in the expected value versus the number n of interpolation points with l_1 error estimator $\tilde{\varepsilon}_j$ for the original SSC without kink information (a), and for the new version with kink information (b).

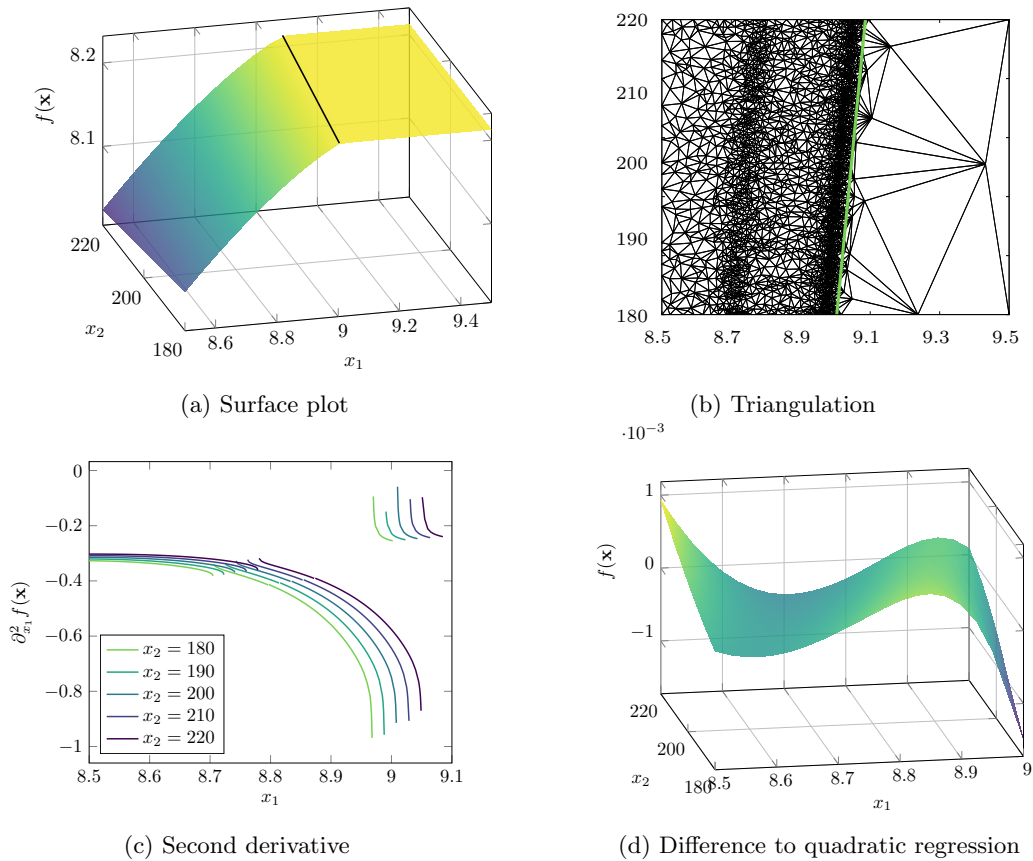


Figure 17: Function $f(\mathbf{x})$ resulting from gas network simulation.

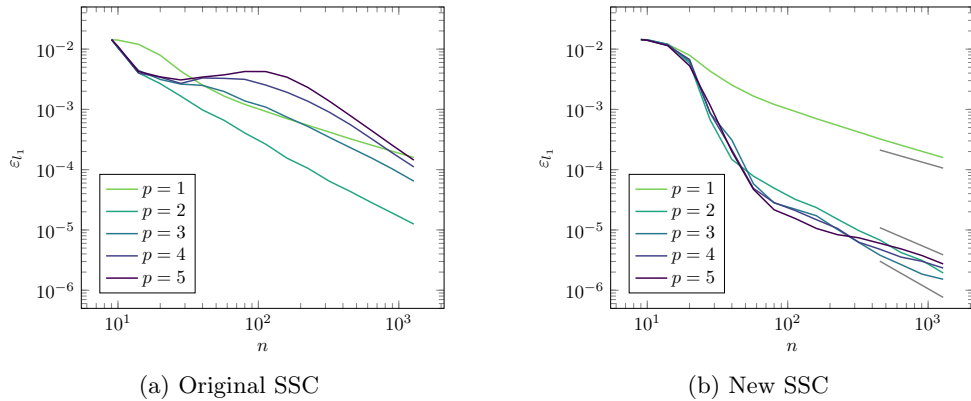


Figure 18: $d = 3$. The l_1 error evaluated at 10^6 random points versus the number n of interpolation points with l_1 error estimator $\tilde{\varepsilon}_j$ for the original SSC without kink information (a), and for the new version with kink information (b).

Because the original version does not have any information about the kink in the function $f(\mathbf{x})$, the convergence rates for polynomial degrees of $p \geq 2$ are the same. The new version has some information about the kink in the function, but no information about the kink in the first derivative (corresponding to the jump in the second derivative) and, therefore, the convergence rates for $p \geq 3$ are the same. At first glance, we only improved the order of convergence from 1.5 to 2, but at second glance, we see that our new simplex stochastic collocation has a significantly better pre-asymptotic behavior. This is due to the fact that the linear and quadratic terms of $f(\mathbf{x})$ contribute most, whereas the higher order terms are only of magnitude 10^{-3} . See Figure 17d for the difference between the function $f(\mathbf{x})$ and a quadratic regression at the left side of the kink.

3.4 Input Uncertainties in Three Dimensions

In addition to the first two uncertain parameters, we now add a third one. The power x_3 of the withdrawn gas at the marked demand node is uniformly varied between 230 MW and 250 MW. See Figure 18a for the error of the original stochastic simplex collocation. The best convergence rate is obtained for a polynomial degree of $p = 2$ and increasing the degree results in a larger error estimate. This is not the case for our modified simplex stochastic collocation, see 18b. The error is in the same order of magnitude for all polynomial degrees $p = 2, 3, 4, 5$ and converges with an order of 1. Here, the good pre-asymptotic behavior can be seen even better than in $d = 2$ dimensions. Figure 19 shows the convergence results for the expectation. As in $d = 2$ dimensions, the reference value is computed with the new version of the simplex stochastic collocation, a polynomial degree of five, and $n = 5120$ interpolation points. For the original version (a), the difference between different polynomial degrees is not as large as predicted by the error estimator. The rate is of the same order of magnitude as for the new simplex stochastic collocation (b), but the new version benefits from the explicit kink approximation in the pre-asymptotic. Hence, only $m \approx 50$ instead of $m \approx 200$ sampling points are necessary to obtain an error of 10^{-4} .

3.5 Input Uncertainties in Four Dimensions

Lastly, we add an uncertainty at the power x_4 of the withdrawn gas at the third marked demand node. The power uniformly varies between 10 MW and 30 MW. As in $d = 2$

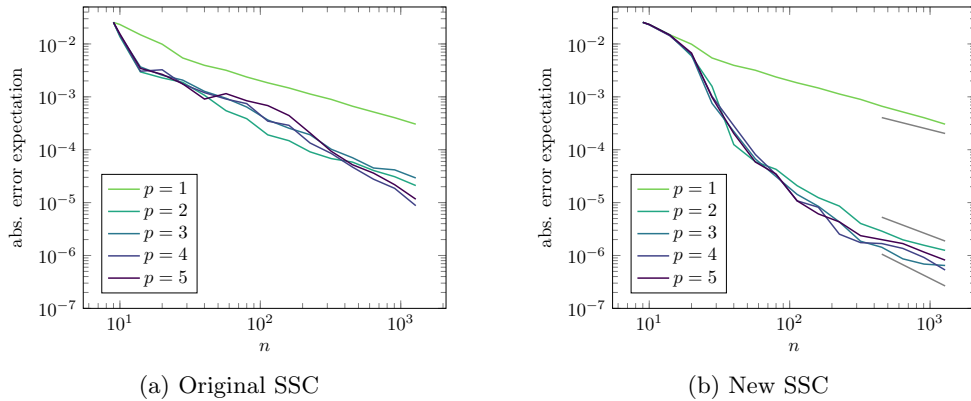


Figure 19: $d = 3$. The absolute error in the expected value versus the number n of interpolation points with l_1 error estimator $\tilde{\varepsilon}_j$ for the original SSC without kink information (a), and for the new version with kink information (b).

and $d = 3$ dimensions, the estimated l_1 error of the original simplex stochastic collocation increases with increasing polynomial degree, see Figure 20a. This difference is no longer visible in the error of the expectation, where all polynomial degrees result in errors of same order of magnitude, see Figure 21a. Again, the new version of the stochastic simplex collocation yields better results because of the better pre-asymptotic behavior. There is no visible benefit from using polynomials of degree $p \geq 3$, but the obtained order of convergence is 1. To achieve an error of 10^{-4} , we only need $m \approx 100$ sampling points, whereas the original version does not reach this error with $m \approx 1000$ sampling points.

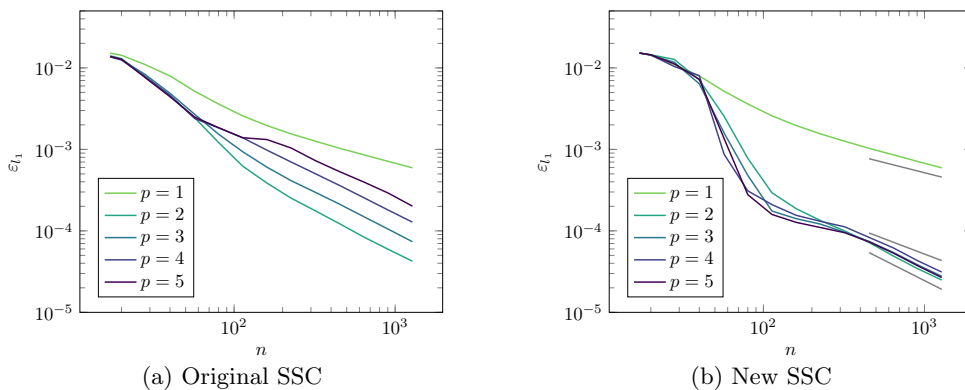


Figure 20: $d = 4$. The l_1 error evaluated at 10^6 random points versus the number n of interpolation points with l_1 error estimator $\tilde{\varepsilon}_j$ for the original SSC without kink information (a), and for the new version with kink information (b).

3.6 Comparison to Other Methods

Finally, we compare our new simplex stochastic collocation method with other common integration methods for computing an expected value. The convergence plots are shown in Figure 22 for dimensions $d = 2$, $d = 3$, and $d = 4$. The Monte Carlo quadrature does not

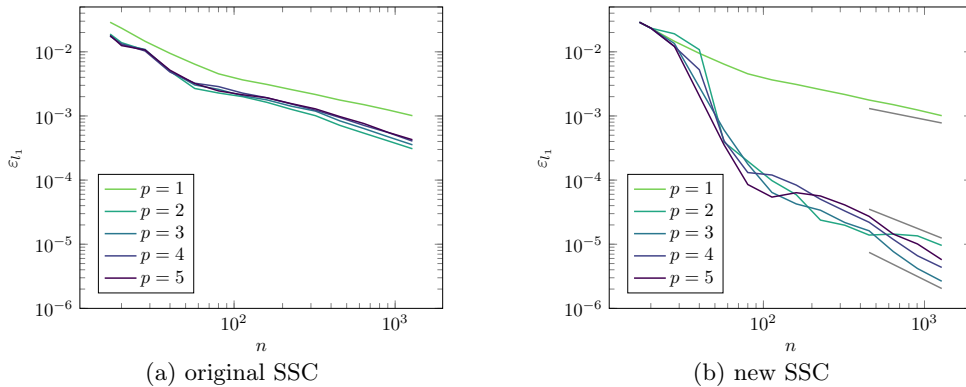


Figure 21: $d = 4$. The absolute error in the expected value versus the number n of interpolation points with l_1 error estimator $\tilde{\varepsilon}_j$ for the original SSC without kink information (a), and for the new version with kink information (b).

make any requirements on the integrand, therefore, the theoretical order of convergence of $1/2$ is obtained in all dimensions. The quasi-Monte Carlo quadrature [11] rule with Halton points [7, 12] yields better results. In $d = 2$ and $d = 3$ dimensions an order of approximately 1 is reached, whereas in $d = 4$ dimensions the order is only $3/4$. For sufficiently smooth integrands, sparse grid quadrature provides even better convergence. Since the considered integrand here is only in $\mathcal{C}^0(\Omega)$, it is quite interesting how well sparse grids perform. We use a regular and a spatially adaptive sparse grid [13, 14] with polynomials of degree five. The spatially adaptive variant allows you to place more points near singularities or discontinuities [8]. In $d = 2$ dimensions, both sparse grids yield better results than the quasi-Monte Carlo quadrature, but with the same order of convergence of 1. Here, the spatially adaptive sparse grid is slightly better than the regular one. In $d = 3$ dimensions, both sparse grid quadratures are still better than the quasi-Monte Carlo quadrature but in the end, the adaptively added points yield worse results. In $d = 4$ dimensions, the regular sparse grid completely fails, and the spatially adaptive sparse grid is only as good as the quasi-Monte Carlo quadrature. In all dimensions, we get the best results with the simplex stochastic collocation. In $d = 2$ dimensions the maximal obtained order of convergence 2 is twice as good as the one for sparse grids and quasi-Monte Carlo quadrature. Additionally, the pre-asymptotic is also better. In $d = 3$ and $d = 4$ dimensions, the convergence rate of the simplex stochastic collocation is the same, but, again, the better pre-asymptotic makes a difference. Concluding, we can say that the explicit kink approximation is useful and worthwhile, even though the theoretical convergence rates are not obtained due to the jumps in the second derivative. All methods requiring a certain smoothness suffer from these jumps.

4 Conclusion

We introduced an approach of simplex stochastic collocation for a piecewise approximation of a function with polynomials of degree p , where the function is not continuously differentiable and has kinks. By using a-posteriori information, which incorporates application knowledge, we could explicitly approximate the kink, which yields significantly better results. We proved that this modification results in algebraic orders of convergence of $(p+1)/d$ and verified the rates with test functions in $d = 2, 3, 4$ dimensions. Moreover, we introduced two new error estimators for an adaptive refinement. We showed that in contrast to the original error

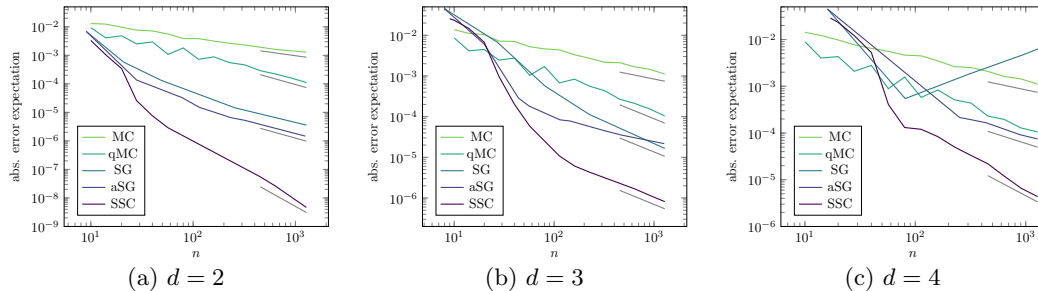


Figure 22: The absolute error of the expected value versus the number n of interpolation points for Monte Carlo integration, quasi-Monte Carlo integration with the Halton sequence, regular sparse grids, spatially adaptive sparse grids, and simplex stochastic collocation with a polynomial degree of five.

estimators, our ones were reliable and solution-based without incorporating unnecessary simulation runs. For multiple refinements, as proposed in [20, 21, 22], we analyzed the error distribution over the simplices and showed that this approach is reasonable and does not affect the convergence rates.

We applied our improved version of simplex stochastic collocation to a real gas network. Due to the empirical behavior of the employed gas network simulator, which resulted in jumps in the second partial derivative of the quantity of interest due to numerical reasons, we could not reach the desired convergence rates for the quantity of interest. Nevertheless, we saw that even in $d = 4$ dimensions only 100 sampling points were necessary to approximate an expected value as accurate as the model error of 10^{-4} . A comparison with other common methods, such as sparse grid and (quasi-) Monte Carlo quadrature, showed that our method benefits from the explicit kink approximation and, hence, yields significantly better results.

So far, we have used the simplex stochastic collocation only for random variables that were uniformly distributed. Therefore, the next canonical step will be to extend the method of simplex stochastic collocation for random variables following other distributions with bounded support. Instead of weighting an error estimator with the area of a simplex, the error estimator could be weighted with the probability of a simplex. This idea was already presented for the original version of stochastic simplex collocation [20, 21, 22] and should not cause any problems. The more interesting question is whether simplex stochastic collocation can be used for random variables whose density function has unlimited support and how bounding the support influences the method.

Furthermore, we have seen that the method of Voronoi piecewise surrogate models [15] provided better convergence results than simplex stochastic collocation for functions with many local minima and maxima. This could be due to the fact that, in Voronoi piecewise surrogate models, the approximation is based on solving a regression problem over the $2P$ -nearest neighbors of each cell instead of solving an interpolation problem over the P -nearest neighbors. Therefore, it should be investigated how the use of regression affects simplex stochastic collocation and whether it improves its convergence.

Acknowledgement

This work is funded by the German Federal Ministry for Economic Affairs and Energy (BMWi) within the project MathEnergy.

A Appendix

A.1 Generation of Random Points in Simplices

According to [3], an efficient way to sample uniform distributed random points in the unit simplex

$$S_d = \left\{ (s_1, \dots, s_d) : s_i \geq 0, \sum_{i=1}^d s_i \leq 1 \right\} \quad (10)$$

is the following. Let u_1, u_2, \dots, u_{d+1} be independent and identically uniform in $[0, 1]$ distributed random numbers. Then the random variables $e_1 = -\log(u_1), e_2 = -\log(u_2), \dots, e_{d+1} = -\log(u_{d+1})$ are independent and identically exponentially distributed with parameter $\lambda = 1$. Let $s = \sum_{i=1}^{d-1} s_i$, then the vector

$$\mathbf{x} = (x_1, x_2, \dots, x_d) = (e_1/s, e_2/s, \dots, e_d/s) \quad (11)$$

is uniform distributed in simplex S_d . This method has the advantage that no sample points must be rejected nor a sorting of numbers is required.

References

- [1] T. Clees, K. Cassirer, N. Hornung, B. Klaassen, I. Nikitin, L. Nikitina, R. Suter, and I. Torgovitskaia. MYNTS: Multi-physics network simulator. In *Proceedings of the 6th International Conference on Simulation and Modeling Methodologies, Technologies and Applications*, pages 179–186, 2016.
- [2] I. Colombo, F. Nobile, G. Porta, A. Scotti, and L. Tamellini. Uncertainty Quantification of geochemical and mechanical compaction in layered sedimentary basins. *Computer Methods in Applied Mechanics and Engineering*, 328:122–146, jan 2018.
- [3] L. Devroye. *Non-uniform random variate generation*. Springer, New York, 1986.
- [4] B. Fuchs. *Numerical Methods for Uncertainty Quantification in Gas Network Simulation*. PhD thesis, University of Bonn, 2018. URN: urn:nbn:de:hbz:5n-52014.
- [5] M. Griebel, F. Kuo, and I. Sloan. The smoothing effect of integration in \mathbb{R}^d and the ANOVA decomposition. *Mathematics of Computation*, 82:383–400, 2013.
- [6] M. Griebel, F. Kuo, and I. Sloan. Note on "The smoothing effect of integration in \mathbb{R}^d and the ANOVA decomposition". *Mathematics of Computation*, 86:1855–1876, 2017.
- [7] J. Halton. On the efficiency of certain quasi-random sequences of points in evaluating multi-dimensional integrals. *Numerische Mathematic*, 2:84–90, 1960.
- [8] J. Jakeman, R. Archibald, and D. Xiu. Characterization of discontinuities in high-dimensional stochastic problems on adaptive sparse grids. *Journal of Computational Physics*, 230(10):3977–3997, 2011.
- [9] T. Koch, B. Hiller, M. Pfetsch, and L. Schewe. *Evaluating Gas Network Capacities*. Society for Industrial and Applied Mathematics, Philadelphia, PA, 2015.
- [10] M. Lurie. *Modeling of Oil Product and Gas Pipeline Transportation*. Wiley-VCH Verlag GmbH and Co. KGaA, Weinheim, Germany, 2008.

- [11] H. Niederreiter. *Random Number Generation and Quasi-Monte Carlo Methods*. Society for Industrial and Applied Mathematics, 1992.
- [12] A. Owen. Halton sequences avoid the origin. *SIAM Review*, 43(3):487–503, 2006.
- [13] D. Pflüger. *Spatially Adaptive Sparse Grids for High-Dimensional Problems*. Verlag Dr. Hut, München, 2010.
- [14] D. Pflüger. Spatially adaptive refinement. In J. Garcke and M. Griebel, editors, *Sparse Grids and Applications*, Lecture Notes in Computational Science and Engineering, pages 243–262, Berlin Heidelberg, 2012. Springer.
- [15] A. Rushdi, L. Swiler, E. Phipps, M. D’Elia, and M. Ebeida. VPS: Voronoi piecewise surrogate models for high-dimensional data fitting. *International Journal for Uncertainty Quantification*, 7(1):1–21, 2017.
- [16] K. Sargsyan, C. Safta, B. Debusschere, and H. Najm. Uncertainty Quantification given Discontinuous Model Response and a Limited Number of Model Runs. *SIAM Journal on Scientific Computing*, 34(1):B44–B64, jan 2012.
- [17] T. Sauer and Y. Xu. A case study in multivariate Lagrange interpolation. In S. Singh, editor, *Approximation Theory, Wavelets and Applications*, pages 443–452. Springer, Dordrecht, 1995.
- [18] M. Schmidt, M. Steinbach, and B. Willert. High detail stationary optimization models for gas networks: validation and results. *Optimization and Engineering*, 17(2):437–472, 2016.
- [19] R. C. Smith. *Uncertainty Quantification: Theory, Implementation, and Applications*. SIAM, 2014.
- [20] J. Witteveen and G. Iaccarino. Refinement criteria for simplex stochastic collocation with local extremum diminishing robustness. *SIAM Journal on Scientific Computing*, 34(3):A1522–A1543, 2012.
- [21] J. Witteveen and G. Iaccarino. Simplex stochastic collocation with random sampling and extrapolation for nonhypercube probability spaces. *SIAM Journal on Scientific Computing*, 34(2):814–838, 2012.
- [22] J. Witteveen and G. Iaccarino. Simplex stochastic collocation with ENO-type stencil selection for robust uncertainty quantification. *Journal of Computational Physics*, 239:1–21, 2013.